Developmental Biology
April 2016, Volume 412 Issue 2 Pages 298-310
https://doi.org/10.1016/j.ydbio.2016.02.026
https://archimer.ifremer.fr/doc/00371/48249/

ROCK inhibition abolishes the establishment of the aquiferous system in *Ephydatia muelleri* (Porifera, Demospongiae)

Schenkelaars Quentin [1, 2, *], Quintero Omar [3], Hall Chelsea [3], Fierro-Constain Laura [1], Renard Emmanuelle [1], Borchiellini Carole [1], Hill April L. [3, *]

[1] Aix Marseille Univ, Inst Mediterraneen Biodiversite & Ecol Marine & C, UAPV, CNRS,UMR 7263,IRD 237, Marseille, France.
[2] Univ Geneva, Fac Sci, Inst Genet & Genom Geneva IGe3, Dept Genet & Evolut, CH-1211 Geneva 4, Switzerland.
[3] Univ Richmond, Dept Biol, Richmond, VA 23173 USA.

* Corresponding authors : Quentin Schenkelaars, email address : quentin.schenkelaars@unige.ch ; April L. Hill, email address : ahill2@richmond.edu

Abstract :

The Rho associated coiled-coil protein kinase (ROCK) plays crucial roles in development across bilaterian animals. The fact that the Rho/Rock pathway is required to initiate epithelial morphogenesis and thus to establish body plans in bilaterians makes this conserved signaling pathway key for studying the molecular mechanisms that may control early development of basally branching metazoans. The purpose of this study was to evaluate whether or not the main components of this signaling pathway exist in sponges, and if present, to investigate the possible role of the regulatory network in an early branching non-bilaterian species by evaluating ROCK function during Ephydatia muelleri development. Molecular phylogenetic analyses and protein domain predictions revealed the existence of Rho/Rock components in all studied poriferan lineages. Binding assays revealed that both Y-27632 and GSK429286A are capable of inhibiting Em-ROCK activity in vitro. Treatment with both drugs leads to impairment of growth and formation of the basal pinacoderm layer in the developing sponge. Furthermore, inhibition of Em-Rock prevents the establishment of a functional aquiferous system, including the absence of an osculum. In contrast, no effect of ROCK inhibition was observed in juvenile sponges that already possess a fully developed and functional aquiferous system. Thus, the Rho/Rock pathway appears to be essential for the proper development of the freshwater sponge, and may play a role in various cell behaviors (e.g. cell proliferation, cell adhesion and cell motility). Taken together, these data are consistent with an ancestral function of Rho/Rock signaling in playing roles in early developmental processes and may provide a new framework to study the interaction between Wnt signaling and the Rho/Rock pathway.

Highlights

► *Bona fide* components of the Rho/Rock pathway were identified in sponges. ► Y-27632 and GSK429286A inhibitors reduce the kinase activity of Em-ROCK *in vitro*. ► Early hatching gemmules treated with ROCK inhibitors show abnormal growth. ► Em-ROCK inhibition leads to the lack of aquiferous system. ► A cross-talk between Wnt, Rho/Rock and JNK/JUN is proposed here.

Keywords : Porifera, Ephydatia muelleri, ROCK, Development, Y-27632, GSK429286A, Morphogenesis

Introduction

Understanding the origin and evolution of the molecular mechanisms that underlie animal development is a fundamental goal in evolutionary developmental biology. Even though the order and relationship of the basal metazoans is still controversial, poriferans remain as one of the earliest branching animal lineages (Dohrmann and Worheide, 2013; Nosenko et al., 2013; Philippe et al., 2009; Pick et al., 2010; Pisani et al., 2015; Ryan et al., 2013). Furthermore, multiple lines of evidence suggest that early animals possessed poriferan-like body plans, and thus, extant sponges may provide key knowledge about the origins of complex animal bodies (Leininger et al., 2014). Though sponges are structurally simple organisms, they have a very similar complement of molecular machinery to other animals and possess genes that may be used to set up pathways for growth, differentiation, cell specification, adhesion, and sensory function (Leys and Hill, 2012). Sponges mainly consist of a matrix (the mesohyl) encompassed between two epithelial layers of flagellated cells (i.e.

the exopinacoderm and the endopinacoderm). Briefly, the exopinacoderm refers to sponge external surface while the endopinacoderm lines the internal aquiferous system (i.e. canals and choanocyte chambers). Leys and Hill (2012) reviewed many features of pinacoderms which are consistent with epithelial structure including junctions that hold cells together (adherens and occluding junctions), polarized cells (T-shaped cells with the nucleus in a cell body that projects down into the collagenous middle layer), the coating proteoglycan matrix and the fact that these thin single layers of cells can and do form effective barriers (Adams et al., 2010). Interestingly, body shape of sponges is mainly organized by the aquiferous system (i.e. canals, osculum and choanocyte chambers) and thus depends on pinacoderm morphogenesis whereas a skeleton of spicules supports the whole structure (Renard et al., 2013). Importantly, poriferan anatomy and physiology relies on the aquiferous system and it is commonly accepted that the sponge body plan is formed by the establishment of this structure (Windsor and Leys, 2010).

The acquisition of the *Amphimedon queeslandica* (Porifera, Demospongiae) genome (Srivastava et al., 2010, 2008) shed light on the origin and evolution of several key conserved signaling pathways, such as Wnt, Notch, and TGF-β (Adamska et al., 2010, 2007; Fahey and Degnan, 2010; Gazave et al., 2009; Richards and Degnan, 2009). Although the growing accumulation of genomic and transcriptomic databases of early divergent phyla has increased our knowledge of the ancestral molecular toolkit of animals (Fortunato et al., 2015; Leininger et al., 2014; Moroz et al., 2014; Nichols et al., 2006; Pang et al., 2010; Riesgo et al., 2014; Ryan et al., 2013), functional studies elucidating roles for the conserved animal specific signaling pathways remain scarce, especially in the Porifera. Of note, recent studies have focused on the role the Wnt pathway plays in body plan patterning in these basally branching metazoans (Adamska et al., 2010, 2007; Pang et al., 2010). For example, activation of the Wnt pathway in *Ephydatia muelleri* by lithium chloride or alsterpaullone leads to formation of

ectopic oscula and disruption of aquiferous system function supporting the hypothesis that Wnt signaling determines body axis polarity in freshwater sponges (Windsor and Leys, 2010). However, the molecular mechanisms that control morphogenesis during aquiferous system establishment are not well understood.

The Rho/Rock pathway has been recognized for its function in cytoskeletal dynamics and thus in cell shape, cell adhesion and cell migration, as well as involvement in non-canonical Wnt signaling in bilaterians (Amano et al., 2010; Schlessinger et al., 2009). Several downstream substrates of Rho-kinase (ROCK) such as the myosin regulatory light chain (MRLC) of myosin II and Lim kinase (LIMK) have been identified as key regulatory components of the cytoskeleton (Winter et al., 2001). The MRLC mediates actomyosin contractility whereas LIMK is responsible for the turnover of actin filaments (Maekawa, 1999; Watanabe et al., 2007). The implication of ROCK substrates in cytoskeleton reorganization has given rise to studies focused on ROCK function in the context of tissue morphogenesis during bilaterian development. Indeed, by inducing apical cell constriction through actomyosin contractility, Rho/Rock signaling plays major roles in the establishment of bottle cells and thereby allows the initiation of key developmental stages relying on invagination (Mason et al., 2013; Sherrard et al., 2010; Zimmerman et al., 2010). For instance, ROCK activity is necessary for the proper placement of the apical cytoskeleton during lens placode invagination in chick and mouse (Borges et al., 2011; Chauhan et al., 2011; Plageman et al., 2011), and invagination of salivary glands in *Drosophila* (Xu et al., 2008). As well, many other morphogenetic processes during embryogenesis rely on Rho/Rock activity (Escuin et al., 2015; Lee et al., 2006; Reed et al., 2009; Stankova et al., 2015; Verdier et al., 2006) such as extension/convergent movements during *Xenopus* gastrulation (Habas et al., 2001; Kim and Han, 2005). Although the Rho/Rock pathway has been described as an essential molecular signaling pathway for morphogenetic processes across Bilateria, the

existence and the underlying role of this module in early branching animal lineages such as Porifera has yet to be elucidated.

Given the important connection of the Rho/Rock module to Wnt signaling and body plan formation in bilaterians, we asked if and how the Rho/Rock pathway is functioning in Porifera. The goal of this study was to determine if the Rho/Rock pathway is involved in sponge aquiferous system development and if ROCK plays roles in setting up the body plan in sponges as it does in bilaterians.

Results & Discussion

Orthologous genes of the Rho/Rock pathway in sponges

We have examined whether the main components of the Rho/Rock pathway are present in different sponge lineages. Orthologs for *rho, rock, mrlc* and *limk* were identified in Demospongia (*Amphimedon queenslandica* and *Ephydatia muelleri*), Homoscleromorpha (*Oscarella lobularis* and *Oscarella sp.*), Calcarea (*Sycon ciliatum*) and Hexactinellida (*Aphrocallistes vastus* and *Oopsacas minuta*) (Table S1 to S8). Phylogenetic analysis supports that sponge sequences belong to each subfamily using both ML and Bayesian methods (Figure 1, S1 and S2) and all functional domains were predicted for RHO, MRLC and LIMK (except for LIMK in *Oscarella* genus) (Figure S3 to S5).

All poriferan ROCK sequences possessed the protein kinase (PK) domain and the AGC kinase C-terminal domain (except for one of the Sycon orthologs, ScRockB). The Rho-binding domain (or its corresponding G3DSA:1.20.5.730 InterProScan domain) required for RHO-ROCK interaction in bilaterians was predicted for *Amphimedon queenslandica* (Demospongiae), *Oopsacas minuta* (Hexactinelida), *Sycon ciliatum* (Clacarea), *Oscarella lobularis* and *Oscarella carmela* (Homoscleromorpha) (Figure 2). Retrieving this domain in

147 sequences from the four poriferan lineages strongly suggests that it is an ancestral feature of
148 ROCK proteins, and that its apparent absence in *Aphrocalistes vastus* (Hexactinellida),
149 *Ephydatia muelleri* (Demospongiae) and *Oscarella sp.* (Homoscleromorpha) is likely due to
150 limits in software prediction. In accordance with this interpretation, an identical motif to the
151 Rho-binding motif identified in vertebrates was found in *S. ciliatum* (LKxxAVNKLAxxV), *O.*
152 *lobularis* and *O. carmela* (LKxxAVNKLAxxM) (Figure S6) (Dvorsky, 2003). Further, a more
153 divergent motif was retrieved in *A. queenslandica* (MKxxAINKLxxxM), *E. muelleri*
154 (LKxxxxITKLxxxL), *O. sp.* (LKxxAVNKLxxxM), *A. vastus* and *O. minuta*
155 (LKxxAIxKLxxxx). Thus, even if some motifs have diverged, it is probable that the RHO-
156 ROCK interaction has been maintained from sponges to vertebrates.

157 The Pleckstrin homology domain (PH), however, required for membrane location of
158 the protein in bilaterians (Dvorsky, 2003; Tu et al., 2011), was retrieved only in *Oscarella*
159 genus (Figure 2). In contrast, other sequences found in sponges contain the DAG domain (or
160 its corresponding G3DSA:3.30.60.20 InterProScan domain), which is also involved in
161 membrane binding. Although a lack of domain prediction could be attributed to software
162 limitations for detecting divergent sequences, *Oscarella* sequences clearly miss the segment
163 containing the C-terminal cysteine pattern corresponding to DAG domain and thus share a
164 more conventional PH domain instead of the characteristic split PH domain found in other
165 species (Figure S6). This finding suggests that ROCK regulation at the cell membrane may
166 occur in a different manner in corresponding species or that more variability exists in PH
167 domain sequences than has been accounted for by prediction algorithms.

168 Given that i) the key proteins of the Rho/Rock pathway are present across sponge
169 lineages and that ii) their respective functional domains share important structural features as
170 described in bilaterians, it seems likely that the Rho/Rock pathway is part of an ancestral and
171 conserved toolkit of the Metazoa.

Rock expression during freshwater sponge development

We next asked whether or not Rock is expressed during early sponge development in the model sponge system, *Ephydatia muelleri*. Freshwater sponge development from gemmules is divided into five main stages (Figure S7; after (Funayama et al., 2005)). Stage 1 corresponds to gemmule hatching and attachment to the substrate whereas stage 2 and 3 lead to cell proliferation in two and three dimensions. Finally, after choanocyte chamber formation at stage 3, stage 4 corresponds to the early development of an aquiferous system and stage 5 is recognizable by the presence of a functional aquiferous system (with osculum). Analyses by qRT-PCR showed that *Em-Rock* is expressed at a low level (less than $8.0*10^{-5}$ arbitrary unit: a.u) during gemmule hatching (stage 1), followed by a higher level ($1.1*10^{-4}$ a.u) of expression over the course of development from stage 2-4 (Figure 3). Finally *Em-rock* expression was 3 fold higher at aquiferous system establishment (stage 5) than at stage 1. Thus, *Em-Rock* is expressed from the onset of gemmule hatching and increases during later stages of development. Consequently, it appears that the *Rock* gene is involved in early development and perhaps morphogenesis of sponges at least until aquiferous system establishment in juveniles.

Testing ROCK kinase activity and the efficacy of ROCK inhibitors in vitro

Y-27632 and GSK429286A are two highly selective inhibitors targeting ROCK by competing with ATP binding (Davies et al., 2000; Ishizaki et al., 2000; Nichols et al., 2009). However, most studies using these drugs were performed on vertebrates. To determine if the Em-ROCK kinase domain displays kinase activity and if, both inhibitors inhibit Em-ROCK, we purified and tested the bacterially expressed Em-ROCK kinase domain (Figure 4A). In

order to do so, after double purification (Figure 4B), the enzymatic activity of FLAG-Em-ROCK-6xHis was monitored in absence of either drug (Figure 4C). It appears that Em-ROCK activity increased linearly with Em-ROCK concentration (R=0.991) when FLAG-GFP-6xHis similarly purified showed no activity in the ROCK assay (not shown here). The inhibitory activity of each drug was experimentally tested in the presence of increased concentrations of inhibitors. We found that both inhibitors inhibit Em-ROCK activity *in vitro* (Figure 4D). Of note, Em-ROCK activity was more effectively reduced by Y-27632 than the GSK429286A. While Y-27632 inhibited Em-ROCK with IC_{50} of 10µM, GSK429286A reduced Em-ROCK activity with IC_{50} of 100µM. According to the manufacturer, Y-27632 inhibits mammalian ROCK I and ROCK II with IC_{50} of 140nM and 300nM respectively, whereas GSK429286A is a more efficient inhibitor with IC_{50} of 14nM and 63nM, respectively. This means that higher concentration of Y-27632 and GSK429286A is needed to effectively inhibit Em-ROCK *in vivo*. However, a large number of studies aiming to understand ROCK function frequently used Y-27632 at 10µM with very low off target effects (Cheng et al., 2015; Davies et al., 2000; Harb et al., 2008; Huh et al., 2013; Kanthou, 2002; Okumura et al., 2009). In contrast, few data are currently available for GSK429286A inhibitor but it has been previously used at 1µM (Nichols et al., 2009).

ROCK inhibition induced abnormal growth of sponges

Incubation of early stage sponges with 1, 5, 10 or 20µM of Y-27632 over the course of 24 hours led to alterations of the leading edge of sponge growth compared to control sponges at the same developmental stage (Figure 5A and B). Instead of having a roughly circular shape around the growing epithelial pinacodermal growth zone (n=48/53), gemmules treated with Y-27632 routinely showed multiple outgrowths at points around the leading edge of

epithelial development of the basal pinacoderm (n=165/169) (Figure 5B). We implemented a Uniform Growth Index (UGI), which permitted us to quantify growth disturbance of the leading edge (Figure S8). Analyses support that each tested concentration of Y-27632 was sufficient to significantly affect the edge growth zone (p-values < 0.0001) while no significant differences in UGI average were evident by increasing drug concentration (Figure 6). Hence, whereas control sponges had a UGI of 1.0, the average in treated gemmules was approximately 1.6 even at 1µM.

Interestingly, 30% of sponges treated with 10µM (n=10) or 25µM (n=11) of GSK429286A demonstrated growth zone aberrations after 24 hours as well (Figure 7A and B). In addition, all sponges cultivated at the highest concentration (n=13) also exhibit abnormal body shape of the basal pinacoderm (Figure 7A and B). Changes in the growth zone resulted in flattened, expanded and non-circular body shape at lowest concentrations (10µM and 25µM) when small outgrowths were observed at the highest concentration (50µM). When compared to the results obtained with Y-27632, it appears that a dose dependent effect is observed when GSK429286A was used.

The variability in phenotypes after 24 hours observed when comparing Y-27632 (Figure 5B) and GSK429286A (Figure 7B) treatments may suggest that some resulting phenotypes could be off target effects. Indeed, several AGC protein kinases were identified in *E. muelleri* implying that it is possible that either of the drugs may lead to the inhibition of some of these kinases when a high concentration is applied. However, this interpretation is not necessarily supported by the known roles of these specific inhibitors in mammalian systems (Davies et al., 2000), and the high conservation of the targeted protein kinase domain (sequence identity higher than 73% between human paralogs and Em-ROCK). Moreover, off target effects does not explain why even small concentrations of Y-27632 led to the abnormal outgrowths. Furthermore, although phenotypes obtained with each drug appeared slightly

different in the forming basal pinacoderm, both sets of phenotypes suggest a similar mechanism that leads to the high disturbance in growth zone observed. Outgrowths of tissue (Figure 5B and 7B) and expansion of the growth zone (Figure 7B) are consistent with growing evidence that ROCK is a major component involved in cell junctions, cell adhesion, cell migration and cell cycle during morphogenesis in other animals (Anderson et al., 2002; Harb et al., 2008; Okumura et al., 2013, 2009; Riento and Ridley, 2003; Yu et al., 2012). Indeed, numerous studies have begun to shed light on the central molecular cascades that implicate Rho/Rock signaling in mediating cell proliferation and cell migration in different contexts, including cancer formation and metastasis (Bikkavilli et al., 2008; Podar et al., 2007; Potin et al., 2007; Semenov et al., 2007; Shaulian and Karin, 2001). For instance, it appears that the JNK/JUN cascade can compete with ROCK for RHO binding in order to enhance cell proliferation (Figure 8) (Schulte, 2010; Semenov et al., 2007). Yu et al., showed that Y-27632 promotes cell proliferation and cycle progression through Cyclin D1 in astrocytes from the spinal cord of rats (Yu et al., 2012). Thus, it is interesting to observe higher expression of *Em-cyclin D* in treated sponges (+70% of control, Figure 9). However, further studies are needed to unravel if JNK, JUN and CCND do take part in the mechanisms that induced the outgrowth phenotypes presented here.

ROCK, an essential component for promoting aquiferous system establishment

After cultivating gemmules in Strekal's Media (SM) over the course of 48h (n=53) and 72h (n=39), 79% and 95% of sponges exhibited a complete aquiferous system with choanocyte chambers, canals and osculum (Figure 5B and C). In contrast, even if reduced choanocyte chambers and spicules were found (Figure 5B), neither canals nor osculum were observed in any treated sponges (n=169), even at lowest concentrations of Y-27632 (Figure 5C). Moreover, whereas few sponges with osculum were observed at the lowest concentration

of GSK429286A (40% and 10% after 48h and 72h, respectively), no oscula were observed in sponges cultivated with 25µM and 50µM (Figure 7B and C). Accordingly, it appears that ROCK protein is essential for the establishment of the aquiferous system.

Interestingly, replacing drug solutions with SM after 72h of treatment allowed the rescue of the wild phenotype with canals and osculum even at 50µM of GSK429286A (Figure S9). Thus, ROCK appears as an essential protein involved in the establishment of aquiferous system during the development of *E. muelleri* sponges. Moreover, transient loss of ROCK activity during early development of sponges from hatched gemmules appears reversible demonstrating the plasticity of these animals.

In order to establish if this protein is also required to maintain the aquiferous system in juvenile sponges, the Y-27632 treatment was performed using young juvenile sponges that already possessed these structures (1 week old sponges hatched from gemmules). Y-27632 treatment did not disturb the juvenile canal system structures over the duration of experiments (3 days) (Figure 10). Indeed, canals, osculum and choanocyte chambers remained intact and functioning in treated juveniles (n=108). In addition, it appears that canals and osculum growth were maintained.

The fact that ROCK inhibition prevented establishment and development of an operational aquiferous system but did not appear to affect the function of the aquiferous system in sponges already possessing fully developed canals and oscula implies that ROCK may play a key role in initiating sponge morphogenesis as it does in bilaterians.

Effects of ROCK inhibition is restricted to morphogenesis processes

Careful examination of cross-sections of treated and control sponges confirmed that treating gemmules at the onset of hatching led to sponges without oscula and canals (Figure 5B). We also observed that though choanocytes chambers appear smaller, choanocytes and

295 spicules are present in treated gemmules (Figure 5B). This implies that different cell types
296 (choanocytes and sclerocytes) were formed, and thus, that cell differentiation occurred despite
297 the ROCK inhibition. Consistent with this observation, the stem-cell marker *piwi* (Alié et al.,
298 2015) was similarly expressed in sponges showing abnormal body shape ($3.74*10^{-7}$ a.u) and
299 in controls ($3.86*10^{-7}$ a.u) (Figure 9), suggesting that ROCK inhibition did not significantly
300 affect the ratio between stem cells (archeocytes) and differentiated cells. This data supports
301 the hypothesis that the absence of oscula observed here are likely due to the disruption of
302 morphogenetic processes and not to a global loss of cell differentiation.
303

304 ## *Y-27632 is a potential specific inhibitor of Em-ROCK*

305 Although the activity, but not specificity of the drugs was tested in this study, some
306 lines of evidence support the specificity of GSK27632 and Y-27632 to Em-ROCK. The
307 potential off target effects of the drugs were already discussed (i.e., high conservation of the
308 kinase domain, specific inhibition in mammalian cells at the concentration used here, similar
309 phenotypes at very low concentration). Another support of the specific effects of these drugs
310 is that GSK429286A had a lower activity *in vitro* and *in vivo*. Indeed, the fact that higher
311 concentration of GSK429286A was needed to obtain comparable phenotypes to Y-27632 is
312 consistent with the inhibitor curves obtained in vitro for each drug on Em-ROCK activity
313 (Figure 4D), confirming that Y-27632 is more efficient in this species. However, we noted
314 that GSK429286A treated sponges seemed less healthy than Y-27632 since extended
315 incubation of sponges with GSK429286A led to the senescence of sponges and budding
316 (Figure S9). Furthermore, healthy phenotypes were observed when young sponges already
317 possessing fully developed canals and oscula were exposed to high concentrations of Y-
318 27632. This points out that the phenotypes observed during early development of gemmules
319 most likely reflect the loss of Em-ROCK activity rather than a toxic effect of the drugs.

Finally, the fact that treated sponges i) possessed differentiated cells and ii) were able to recover and complete development in less than one day after washout also suggests that the drug specifically inhibit Em-ROCK and do not induce an overall toxic effect. Thus, Y-27632 may be a specific inhibitor of ROCK in *E. muelleri* like it is in all animals studied so far.

We further note that the lack of finding a dose dependent effect in vivo for Y-27632 could be due to the fact that a low level of Em-ROCK protein activity is present in these sponges. ROCK activity assays (as described earlier) from lysed sponge cells did not yield enough Em-ROCK activity for detection. This is what led us to purify and bacterially express the Em-ROCK kinase domain. This suggests that even very low concentrations of Y-27632 could be enough to inhibit Em-ROCK activity and induce the loss of morphogenesis. Given that Y-27632 is known to be a competitive inhibitor of ROCK kinase, it could be that we are saturating Em-ROCK with inhibitor, even at our lowest tested concentration of 1µM.

Aquiferous system, Wnt pathway and Rho/Rock module

The Wnt signaling pathway is one of the major developmental modules for patterning animal body plans (Petersen and Reddien, 2009; Schulte, 2010). Several studies focused on this module have highlighted the underlying molecular mechanisms involved in the establishment of sponge aquiferous systems (Figure 8). For instance, activation of the canonical Wnt pathway (WNT/β-catenin pathway) resulted in ectopic oscula formation in *E. muelleri* (Windsor and Leys, 2010) and promoted ostia formation in *O. lobularis* (Lapébie et al., 2009). Hence it appears that the canonical Wnt pathway and the Rho/Rock modules are parts of the molecular toolkit required for the establishment of the aquiferous system in sponges. It has been previously suggested that the Rho/Rock pathway is one the sub-signaling modules downstream of Dishevelled (DVL) recruitment to the cell membrane (Schulte, 2010; Semenov et al., 2007). In this context, it appears that the Dishevelled associated activator of

morphogenesis (DAAM) binds to DVL and RHO to mediate Wnt signaling to the Rho/Rock pathway (Habas et al., 2001) (Figure 8). Interestingly, DAAM protein, containing all required functional domains (Aspenström et al., 2006; Higgs and Peterson, 2005), was retrieved in almost all poriferan databases studied here (Figure S10 and Table S1 to S8). Moreover, *Em-rock*, *Em-dvl* and *Em-daam* appeared to be concomitantly expressed during early sponge development suggesting that perhaps roles observed in bilaterians could also occur in sponges (Figure 3). While this study did not address the upstream involvement of the Wnt pathway in Rho/Rock function, we did address the question of the impact of ROCK inhibition on Wnt pathway gene *Dvl*. Comparison of *Em-Dvl* expression between treated (10µM of Y-27632 during 72h) and untreated sponges showed that the loss of ROCK activity led to knockdown of *Em-Dvl* expression (level dropped down to 36% of the controls) (Figure 9). Thus, it is possible that ROCK inhibition may have led to a negative feedback loop of all Wnt pathways and thus promotes the absence of aquiferous system in treated sponges (Figure 8). Future studies will need to examine the mechanisms that lead to the absence of an aquiferous system and the potential cross-regulation between the canonical Wnt pathway and the Rho/Rock module (Li et al., 2011; Pinzón-Daza et al., 2014).

Conclusion

The goal of this study was to determine if components of the Rho/Rock pathway are present in non-bilaterian species and if ROCK protein may play similar functions to those described in bilaterians. We found that all sponge lineages studied possess key proteins of the Rho/Rock pathway, implying that these proteins were inherited from the last common ancestor of Metazoa. In addition, structural domain analyses suggest that protein interactions described in bilaterians have likely been maintained from sponges to vertebrates. Finally, evidence that the Em-ROCK kinase domain exhibits Rho kinase activity *in vitro* and that

commercially available ROCK inhibitors target sponge Em-ROCK, lend further evidence to the hypothesis that the Rho/Rock pathway is an evolutionarily conserved module in animals.

In vivo assays with ROCK inhibitors applied during the early development of freshwater sponges provide strong evidence that ROCK is important for inducing morphogenesis and setting up sponge body plans (Figure 8). Furthermore, roles for Wnt and Rho-Rock pathways in aquiferous system morphogenesis are suggested. Clearly, however, the precise cellular mechanisms and the regulatory network existing between the Wnt pathway and the Rho/Rock module in sponges remains to be elucidated.

Finally, we suggest that our findings may provide a new framework and system to investigate the potential function of ROCK and JNK/JUN module in cell division and cell adhesion (Figure 8) (Harb et al., 2008; Yu et al., 2012). Indeed, in addition to the outgrowth phenotypes presented here and the over-expression of *Em-ccnD*, we noted that sponges treated with ROCK inhibitors exhibited a 'looser' structure (cells did not seem to adhere as they did in the controls), suggesting that ROCK inhibition may have also led to disturbances in cell adhesion. We hope that recent discoveries from non-bilaterian animals such as *Ephydatia* or *Hydra* may play roles in our future understanding of the evolution of cancer, tumorigenesis and metastasis (Domazet-Lošo et al., 2014).

Materials and Methods

Gemmules collection and storage

Gemmules were collected near Prince William Forest National Park during late fall/early winter and stored in sampling water or cold Strekal's media (SM) at 4°C (Strekal and McDIFFETT, 1974). They were preserved from the light and aerated weekly and water was replaced monthly. Gemmules were picked and then washed with cold 1% hydrogen

peroxide solution and SM just before use.

Sequences identification and assignation

Orthologous genes of those described in bilaterians (i.e. *rho, rock, mrlc, limk* and *daam*) were searched by tblastn analyses (Altschul et al., 1997) against various poriferan database of each poriferan lineage (Table S9): Demospongiae (*Ephydatia muelleri*), Calcarea (Sycon ciliatum), Hexactinellida (*Aphrocalistes vastus* and *Oopsacas minuta*) and Homoscleromorpha (*Oscarella carmela, Oscarella lobularis* and *Oscarella sp.*). Sequence assignations were first confirmed by reverse tblastx (Wall et al., 2003) on NCBI database and domain analyses using Interproscan 5 software (http://www.ebi.ac.uk/). Sequence alignments were performed using Bioedit clustalW function (Thompson et al., 1994). Rho GTPase analysis was restricted to the core Rho domain (i.e. amino acids 5-177 in human RAC1) (Boureux et al., 2006) whereas ROCK analysis was restricted to the PK domain (i.e. amino acids 76-338 in human ROCKI) and the whole MYL proteins were conserved for phylogenetic analyses. Bayesian analyses were carried out using MrBayes v3.2.3 (Huelsenbeck and Ronquist, 2001), with one cold chain and three heated chains until average deviation split frequencies was below 0.01. Maximum likelihood analyses (ML) were performed using ATGC PhyML 3.0 software (http://www.atgc-montpellier.fr/) (Guindon et al., 2010) and branch supports were estimated using 1000 bootstrap re-sampling. According to ProtTest 3.2 (Darriba et al., 2011), the LG substitution model was used for each protein.

RT-qPCR

qRT-PCR experiments were performed in order to monitor *Em-rock, Em-dvl* and *Em-daam* expression over normal development of sponges from hatched gemmules until

aquiferous system establishment (four replicates). As well, the expression of *Em-ccnd* (n=2), *Em-dvl*, (n=3) *Em-piwi* (as control of another function, n=2) and two housekeeping genes (*Em-ef1*, n=3 and *Em-actin*, n=2) (Infante et al., 2008; Rivera et al., 2013) were compared between treated sponges (10µM of Y-27632 for 72h) and sponges grown in SM (control). Prior to RT-qPCR, sponges were collected and stored in RNAlater. mRNA was extracted using QiagenRNeasy® Mini Kit and cDNA was synthetized with SuperScript® III Reverse transcriptase according to protocols provided by manufacturers. Gene expression was assessed by quantitative real-time PCR amplification using Chromo4 Real Time PCR Detector on a BioRad Engine interfacing with Opticon Monitor Software. Briefly, each gene expression was quantified in 20µL reaction mix containing 10µL of SYBR GreenER qPCR Supermix (Invitrogen) and each gene-specific primer at 2µM final concentration (Table S10). Finally, 2µL of cDNA were added to each reaction. Standard curves were generated by several dilutions of PCR product of each target gene (after purification). Thermal cycling profiles for PCR reaction began with a 94°C incubation for 5 min followed by 35 cycles of 94°C for 15s, 56°C for 30s, 72°C for 45s. Finally, each cycle was completed by a signal acquisition. For experiment over normal development of sponges, expression levels were normalized to the *Ef1a* housekeeping gene and threshold values for Ct calculations were selected by hand to optimize efficiency for samples.

Cloning and protein purification

A ROCK construct was generated by PCR amplification of juvenile *Ephydatia muelleri* cDNA with megaprimers designed to insert the kinase domain (amino acids 2-415) between an N-terminal FLAG and C-terminal 6xHis tag in a pET-21a backbone (Geiser et al., 2001). A similar plasmid was generated using eGFP as the insert. The plasmids were validated by sequencing across the entire insertion.

Plasmid DNA containing the ROCK construct was transformed into Rosetta2(DE3)plysS cells for protein expression. An overnight culture was grown from the transformants and then diluted back to the phase of exponential growth in Terrific Broth containing 50μg/ml Carbenecillin and 10μg/ml chloramphenicol, and expression induced with 1mM IPTG. The culture was then allowed to grow overnight at 16℃, gently shaking. To purify the protein, cell pellets were flash frozen using liquid nitrogen and then resuspended in lysis buffer (50mM Tris buffuer, pH 8, 500mM NaCl, 0.05% TritonX-100, 0.5% deoxycholate, 10mM imidazole, 10μg/ml aprotinin, 10μg/ml leupeptin, 1mM PMSF). The resuspended cells were sonicated using a Branson Digital Sonifier 450 (67% duty-ratio, 50% power, 30 seconds) and treated with Lysozyme (100μg/mL) to further support rupturing of the cells. The lysate was cleared by centrifugation (25,000xg, 20 minutes, 4C), and the supernatant incubated with Talon resin and incubated with gentile shaking at 4℃ overnight. The resin was cleared of the lysate by gravity flow and washed with (50mM Tris buffuer, pH 8, 200mM NaCl, 0.05% TritonX-100, 20mM imidazole, 10μg/ml aprotinin, 10μg/ml leupeptin, 1mM PMSF, 2.5% glycerol). Protein was eluted from the resin with (50mM Tris buffuer, pH 8, 200mM NaCl, 0.05% TritonX-100, 250mM imidazole, 10μg/ml aprotinin, 10μg/ml leupeptin, 1mM PMSF, 2.5% glycerol). The eluate was then applied to FLAG resin and incubated at 4℃ with gentile agitation for 2 hrs. The FLAG resin was then washed by gravity flow (50mM Tris pH 8, 200 mM NaCl. 0.05% Triton, 2mM imidazole, 10μg/mL aprotinin, 10μg/mL leupeptin, 1mM PMSF, 2.5% glycerol) and eluted (50mM Tris pH 8, 200mM NaCl, 0.05% Triton, 2mM imidazole, 10 μg/mL aprotinin, 10 μg/mL leupeptin, 1mM PMSF, 2.5% glycerol, 100μg/mL FLAG peptide). Purification was verified by SDS-PAGE and Coomassie staining. Concentration of the purified protein was determined by Bradford assay using bovine serum albumin as a standard.

ROCK Activity Assay

Em-ROCK activity was monitored by measuring the phosphorylation of the physiological substrate of mammalian RO, MYPT1 at Thr696. All experiments were performed in kinase buffer (25mM Tris, pH 7.5, 10mM $MgCl_2$, 5mM Glycerol-2-Phosphate, 0.1mM Na_3VO_4). ATP (2mM) and DTT (10mM) were added to the ROCK samples in the MYPT1 coated wells to initiate the kinase reaction. All reagents and the protocol were supplied in a 96-well ROCK activity assay kit (Cell Biolabs, Inc.). ROCK activity was monitored by measuring absorbance 450nm using a Beckmann Coulter DTX-880 microplate reader. The protein concentration dependence was measured by varying the concentration of the Talon/FLAG double-purified ROCK in the assay across the concentration range of 0.2-10µM (10-500µg/ml). To assay for the activity of the ROCK inhibitors, Y-27632 and GSK429286A, varying concentrations of the inhibitors were added to an assay mixture containing Em-ROCK at a concentration of 2nM (0.1µg/mL).

ROCK inhibition

Gemmules were incubated in 1mL of SM during 2 or 3 days in 12 well plates at room temperature in order to let them hatch on circular glass coverslips. Once hatched, half of the cultivating media was change in order to reached different final concentration of Y-27632 (Enzo Life science) using a 2.5mM stock solution. By doing so, hatched gemmules were immediately cultivated with 0µM (n=53), 1µM (n=30), 2µM (n=15), 5µM (n=45), 10µM (n=44) or 20µM (n=35) of Y-27632 during 48h or 72h. Half of the solutions was changed every day. Similarly, another batch of hatched gemmules were cultivated in 3mL of SM containing 10µM (n=10), 25µM (n=11) and 50µM (n=13) of GSK429286A (Selleckchem)

using 5mM (1:500 dilution) and 42µM stock solutions (1:840 and 1:1680 dilutions) in DMSO or only DMSO as control (1:500 dilution). The same approach was performed on juvenile sponges using Y-27632 ($n_{control}$=10, $n_{treated}$=108). In this case, hatched gemmules were cultivated over one week in SM before Y-27632 treatment to let them form the aquiferous system.

Monitoring of phenotypic changes

Pictures were taken every 24h and some gemmules were fixed for 4µm cross sections using 4% paraformaldehyde and epoxy resin. Pictures of early stage treatments were analyzed using ImageJ software. In order to highlight alterations in the edge of growth zone, we implement a Uniform Growth Index (UGI) as followed, $UGI = (l_t/L_t)/(\sum(l_c/L_c)/n_c)$ where lt and Lt correspond to the minimum and maximum length separating gemmule center from edge of growth zone in treated sponge, lc and Lc corresponds to the minimum and maximum length separating gemmule center from edge of growth zone in control sponges and nc the number sponges in the control condition (Fig S8).

Statistical analyses

Because some sample sizes were small in the contingency table comparing the number of sponges showing abnormal body shape between treated and untreated sponges, Fisher's exact tests were performed. For the same reason, Fisher's exact tests were also carried out to compare the number of sponges without osculum in each condition.

Shapiro-Wilk and Jarque-Bera normality tests were performed using Microsoft Excel 2007/XLSTAT (version 2014.1.05, Addinsoft) to determine data distribution of UGI. Since UGI data were not normally distributed, we analyzed them using the Kruskal-Wallis one-way

analysis together with a Steel-Dwass-Critchlow-Fligner procedure.

Finally, for *rock*, *dvl* and *daam* a Friedman test and a Nemenyi procedure were used to discriminate stages in gene expression (p_{rock} = 0.006; p_{dvl}=0.006 p_{daam}=0.003 and n=4) over the course of development.

Acknowledgment

We thank Dr S. P. Leys for providing us *Ephydatia muelleri* transcriptomic database and acknowledge NSF/EDEN grant number IOS # 0955517 for providing us the opportunity to enhance new collaborations between the University of Richmond and the Mediterranean Institute of marine and terrestrial Biodiversity and Ecology that allowed this experimental study. We also would like to thank C. A. Davis for her valuable help and availability concerning the microscopy and imaging and F. Gomez for his help. We also acknowledge NIH/NCI grant K01CA160667 to OQ and HHMI grant 52007567 for support of CH.

Bibliography

Adams, E.D.M., Goss, G.G., Leys, S.P., 2010. Freshwater Sponges Have Functional, Sealing Epithelia with High Transepithelial Resistance and Negative Transepithelial Potential. PLoS ONE 5, e15040. doi:10.1371/journal.pone.0015040

Adamska, M., Degnan, S.M., Green, K.M., Adamski, M., Craigie, A., Larroux, C., Degnan, B.M., 2007. Wnt and TGF-β Expression in the Sponge Amphimedon queenslandica and the Origin of Metazoan Embryonic Patterning. PLoS ONE 2, e1031. doi:10.1371/journal.pone.0001031

Adamska, M., Larroux, C., Adamski, M., Green, K., Lovas, E., Koop, D., Richards, G.S., Zwafink, C., Degnan, B.M., 2010. Structure and expression of conserved Wnt pathway components in the demosponge Amphimedon queenslandica: Wnt pathway components in Amphimedon queenslandica. Evol. Dev. 12, 494–518. doi:10.1111/j.1525-142X.2010.00435.x

Alié, A., Hayashi, T., Sugimura, I., Manuel, M., Sugano, W., Mano, A., Satoh, N., Agata, K., Funayama, N., 2015. The ancestral gene repertoire of animal stem cells. Proc. Natl. Acad. Sci. 201514789. doi:10.1073/pnas.1514789112

Altschul, S.F., Madden, T.L., Schäffer, A.A., Zhang, J., Zhang, Z., Miller, W., Lipman, D.J., 1997. Gapped BLAST and PSI-BLAST: a new generation of protein database search programs. Nucleic Acids Res. 25, 3389–3402.

Amano, M., Nakayama, M., Kaibuchi, K., 2010. Rho-kinase/ROCK: A key regulator of the cytoskeleton and cell polarity. Cytoskeleton 67, 545–554.

Anderson, S.C., Stone, C., Tkach, L., SundarRaj, N., 2002. Rho and Rho-kinase (ROCK) signaling in adherens and gap junction assembly in corneal epithelium. Invest. Ophthalmol. Vis. Sci. 43, 978–986.

Aspenström, P., Richnau, N., Johansson, A.-S., 2006. The diaphanous-related formin DAAM1 collaborates with the Rho GTPases RhoA and Cdc42, CIP4 and Src in regulating cell morphogenesis and actin dynamics. Exp. Cell Res. 312, 2180–2194. doi:10.1016/j.yexcr.2006.03.013

Bikkavilli, R.K., Feigin, M.E., Malbon, C.C., 2008. Gαo mediates WNT-JNK signaling through Dishevelled 1 and 3, RhoA family members, and MEKK 1 and 4 in mammalian cells. J. Cell Sci. 121, 234–245. doi:10.1242/jcs.021964

560 Borges, R.M., Lamers, M.L., Forti, F.L., Santos, M.F. dos, Yan, C.Y.I., 2011. Rho signaling pathway and
561 apical constriction in the early lens placode. genesis 49, 368–379. doi:10.1002/dvg.20723

562 Boureux, A., Vignal, E., Faure, S., Fort, P., 2006. Evolution of the Rho Family of Ras-Like GTPases in
563 Eukaryotes. Mol. Biol. Evol. 24, 203–216. doi:10.1093/molbev/msl145

564 Chauhan, B.K., Lou, M., Zheng, Y., Lang, R.A., 2011. Balanced Rac1 and RhoA activities regulate cell
565 shape and drive invagination morphogenesis in epithelia. Proc. Natl. Acad. Sci. 108, 18289–18294.
566 doi:10.1073/pnas.1108993108

567 Cheng, Y.-T., Yeih, D.-F., Liang, S.-M., Chien, C.-Y., Yu, Y.-L., Ko, B.-S., Jan, Y.-J., Kuo, C.-C., Sung, L.-Y.,
568 Shyue, S.-K., Chen, M.-F., Yet, S.-F., Wu, K.K., Liou, J.-Y., 2015. Rho-associated kinase inhibitors
569 promote the cardiac differentiation of embryonic and induced pluripotent stem cells. Int. J. Cardiol.
570 201, 441–448. doi:10.1016/j.ijcard.2015.08.118

571 Darriba, D., Taboada, G.L., Doallo, R., Posada, D., 2011. ProtTest 3: fast selection of best-fit models of
572 protein evolution. Bioinformatics 27, 1164–1165.

573 Davies, S., Reddy, H., Caivano, M., Cohen, P., 2000. Specificity and mechanism of action of some
574 commonly used protein kinase inhibitors. Biochem J 351, 95–105.

575 Dohrmann, M., Worheide, G., 2013. Novel Scenarios of Early Animal Evolution--Is It Time to Rewrite
576 Textbooks? Integr. Comp. Biol. 53, 503–511. doi:10.1093/icb/ict008

577 Domazet-Lošo, T., Klimovich, A., Anokhin, B., Anton-Erxleben, F., Hamm, M.J., Lange, C., Bosch,
578 T.C.G., 2014. Naturally occurring tumours in the basal metazoan Hydra. Nat. Commun. 5.
579 doi:10.1038/ncomms5222

580 Dvorsky, R., 2003. Structural Insights into the Interaction of ROCKI with the Switch Regions of RhoA. J.
581 Biol. Chem. 279, 7098–7104. doi:10.1074/jbc.M311911200

582 Escuin, S., Vernay, B., Savery, D., Gurniak, C.B., Witke, W., Greene, N.D.E., Copp, A.J., 2015. Rho
583 kinase-dependent actin turnover and actomyosin disassembly are necessary for mouse spinal neural
584 tube closure. J. Cell Sci. jcs.164574. doi:10.1242/jcs.164574

585 Fahey, B., Degnan, B.M., 2010. Origin of animal epithelia: insights from the sponge genome:
586 Evolution of epithelia. Evol. Dev. 12, 601–617. doi:10.1111/j.1525-142X.2010.00445.x

587 Fortunato, S.A.V., Adamski, M., Adamska, M., 2015. Comparative analyses of developmental
588 transcription factor repertoires in sponges reveal unexpected complexity of the earliest animals. Mar.
589 Genomics. doi:10.1016/j.margen.2015.07.008

590 Funayama, N., Nakatsukasa, M., Hayashi, T., Agata, K., 2005. Isolation of the choanocyte in the fresh
591 water sponge, Ephydatia fluviatilis and its lineage marker, Ef annexin. Dev. Growth Differ. 47, 243–
592 253.

593 Gazave, E., Lapébie, P., Richards, G.S., Brunet, F., Ereskovsky, A.V., Degnan, B.M., Borchiellini, C.,
594 Vervoort, M., Renard, E., 2009. Origin and evolution of the Notch signalling pathway: an overview
595 from eukaryotic genomes. BMC Evol. Biol. 9, 249. doi:10.1186/1471-2148-9-249

596 Guindon, S., Dufayard, J.-F., Lefort, V., Anisimova, M., Hordijk, W., Gascuel, O., 2010. New algorithms
597 and methods to estimate maximum-likelihood phylogenies: assessing the performance of PhyML 3.0.
598 Syst. Biol. 59, 307–321. doi:10.1093/sysbio/syq010

599 Habas, R., Kato, Y., He, X., 2001. Wnt/Frizzled activation of Rho regulates vertebrate gastrulation and
600 requires a novel Formin homology protein Daam1. Cell 107, 843–854.

601 Harb, N., Archer, T.K., Sato, N., 2008. The Rho-Rock-Myosin Signaling Axis Determines Cell-Cell
602 Integrity of Self-Renewing Pluripotent Stem Cells. PLoS ONE 3, e3001.
603 doi:10.1371/journal.pone.0003001

604 Higgs, H.N., Peterson, K.J., 2005. Phylogenetic analysis of the formin homology 2 domain. Mol. Biol.
605 Cell 16, 1–13.

606 Huelsenbeck, J.P., Ronquist, F., 2001. MRBAYES: Bayesian inference of phylogenetic trees.
607 Bioinformatics 17, 754–755. doi:10.1093/bioinformatics/17.8.754

608 Huh, Y.H., Kweon, H.-S., Kitazawa, T., 2013. ROCK inhibitor, Y-27632, reduces FBS-induced structural
609 alteration in organ-cultured mesenteric artery. J. Anal. Sci. Technol. 4, 15.

610 Infante, C., Matsuoka, M.P., Asensio, E., Cañavate, J., Reith, M., Manchado, M., 2008. Selection of
611 housekeeping genes for gene expression studies in larvae from flatfish using real-time PCR. BMC Mol.
612 Biol. 9, 28. doi:10.1186/1471-2199-9-28

613 Ishizaki, T., Uehata, M., Tamechika, I., Keel, J., Nonomura, K., Maekawa, M., Narumiya, S., 2000.
614 Pharmacological properties of Y-27632, a specific inhibitor of rho-associated kinases. Mol. Pharmacol.
615 57, 976–983.

616 Kanthou, C., 2002. The tumor vascular targeting agent combretastatin A-4-phosphate induces
617 reorganization of the actin cytoskeleton and early membrane blebbing in human endothelial cells.
618 Blood 99, 2060–2069. doi:10.1182/blood.V99.6.2060

619 Kim, G.-H., Han, J.-K., 2005. JNK and ROKα function in the noncanonical Wnt/RhoA signaling pathway
620 to regulate Xenopus convergent extension movements. Dev. Dyn. 232, 958–968.
621 doi:10.1002/dvdy.20262

622 Lapébie, P., Gazave, E., Ereskovsky, A., Derelle, R., Bézac, C., Renard, E., Houliston, E., Borchiellini, C.,
623 2009. WNT/β-Catenin Signalling and Epithelial Patterning in the Homoscleromorph Sponge Oscarella.
624 PLoS ONE 4, e5823. doi:10.1371/journal.pone.0005823

625 Lee, J.-Y., Marston, D.J., Walston, T., Hardin, J., Halberstadt, A., Goldstein, B., 2006. Wnt/Frizzled
626 Signaling Controls C. elegans Gastrulation by Activating Actomyosin Contractility. Curr. Biol. 16,
627 1986–1997. doi:10.1016/j.cub.2006.08.090

628 Leininger, S., Adamski, M., Bergum, B., Guder, C., Liu, J., Laplante, M., Bråte, J., Hoffmann, F.,
629 Fortunato, S., Jordal, S., Rapp, H.T., Adamska, M., 2014. Developmental gene expression provides
630 clues to relationships between sponge and eumetazoan body plans. Nat. Commun. 5.
631 doi:10.1038/ncomms4905

632 Leys, S.P., Hill, A., 2012. Chapter one - The Physiology and Molecular Biology of Sponge Tissues, in:
633 Mikel A. Becerro, M.J.U., Manuel Maldonado and Xavier Turon (Ed.), Advances in Marine Biology,
634 Advances in Sponge Science: Physiology, Chemical and Microbial Diversity, Biotechnology. Academic
635 Press, pp. 1–56.

636 Li, L., Tam, L., Liu, L., Jin, T., Ng, D.S., 2011. Wnt-signaling mediates the anti-adipogenic action of
637 lysophosphatidic acid through cross talking with the Rho/Rho associated kinase (ROCK) pathway.
638 Biochem. Cell Biol. 89, 515–521. doi:10.1139/o11-048

639 Maekawa, M., 1999. Signaling from Rho to the Actin Cytoskeleton Through Protein Kinases ROCK and
640 LIM-kinase. Science 285, 895–898. doi:10.1126/science.285.5429.895

641 Mason, F.M., Tworoger, M., Martin, A.C., 2013. Apical domain polarization localizes actin-myosin
642 activity to drive ratchet-like apical constriction. Nat. Cell Biol. 15, 926–936. doi:10.1038/ncb2796

643 Moroz, L.L., Kocot, K.M., Citarella, M.R., Dosung, S., Norekian, T.P., Povolotskaya, I.S., Grigorenko,
644 A.P., Dailey, C., Berezikov, E., Buckley, K.M., Ptitsyn, A., Reshetov, D., Mukherjee, K., Moroz, T.P.,
645 Bobkova, Y., Yu, F., Kapitonov, V.V., Jurka, J., Bobkov, Y.V., Swore, J.J., Girardo, D.O., Fodor, A., Gusev,
646 F., Sanford, R., Bruders, R., Kittler, E., Mills, C.E., Rast, J.P., Derelle, R., Solovyev, V.V., Kondrashov,
647 F.A., Swalla, B.J., Sweedler, J.V., Rogaev, E.I., Halanych, K.M., Kohn, A.B., 2014. The ctenophore

genome and the evolutionary origins of neural systems. Nature 510, 109–114.
doi:10.1038/nature13400

Nichols, R.J., Dzamko, N., Hutti, J.E., Cantley, L.C., Deak, M., Moran, J., Bamborough, P., Reith, A.D.,
Alessi, D.R., 2009. Substrate specificity and inhibitors of LRRK2, a protein kinase mutated in
Parkinson's disease. Biochem. J. 424, 47–60. doi:10.1042/BJ20091035

Nichols, S.A., Dirks, W., Pearse, J.S., King, N., 2006. Early evolution of animal cell signaling and
adhesion genes. Proc. Natl. Acad. Sci. 103, 12451–12456. doi:10.1073/pnas.0604065103

Nosenko, T., Schreiber, F., Adamska, M., Adamski, M., Eitel, M., Hammel, J., Maldonado, M., Müller,
W.E.G., Nickel, M., Schierwater, B., Vacelet, J., Wiens, M., Wörheide, G., 2013. Deep metazoan
phylogeny: When different genes tell different stories. Mol. Phylogenet. Evol. 67, 223–233.
doi:10.1016/j.ympev.2013.01.010

Okumura, N., Koizumi, N., Kay, E.P., Ueno, M., Sakamoto, Y., Nakamura, S., Hamuro, J., Kinoshita, S.,
2013. The ROCK inhibitor eye drop accelerates corneal endothelium wound healing. Invest.
Ophthalmol. Vis. Sci. 54, 2493–2502.

Okumura, N., Ueno, M., Koizumi, N., Sakamoto, Y., Hirata, K., Hamuro, J., Kinoshita, S., 2009.
Enhancement on primate corneal endothelial cell survival in vitro by a ROCK inhibitor. Invest.
Ophthalmol. Vis. Sci. 50, 3680–3687.

Pang, K., Ryan, J.F., Mullikin, J.C., Baxevanis, A.D., Martindale, M.Q., 2010. Genomic insights into Wnt
signaling in an early diverging metazoan, the ctenophore Mnemiopsis leidyi. EvoDevo 1, 10–10.

Petersen, C.P., Reddien, P.W., 2009. Wnt signaling and the polarity of the primary body axis. Cell 139,
1056–1068. doi:10.1016/j.cell.2009.11.035

Philippe, H., Derelle, R., Lopez, P., Pick, K., Borchiellini, C., Boury-Esnault, N., Vacelet, J., Renard, E.,
Houliston, E., Quéinnec, E., Silva, C.D., Wincker, P., Guyader, H.L., Leys, S., Jackson, D.J., Schreiber, F.,

671 Erpenbeck, D., Morgenstern, B., Wörheide, G., Manuel, M., 2009. Phylogenomics Revives Traditional
672 Views on Deep Animal Relationships. Curr. Biol. 19, 706–712. doi:10.1016/j.cub.2009.02.052

673 Pick, K.S., Philippe, H., Schreiber, F., Erpenbeck, D., Jackson, D.J., Wrede, P., Wiens, M., Alie, A.,
674 Morgenstern, B., Manuel, M., Worheide, G., 2010. Improved Phylogenomic Taxon Sampling
675 Noticeably Affects Nonbilaterian Relationships. Mol. Biol. Evol. 27, 1983–1987.
676 doi:10.1093/molbev/msq089

677 Pinzón-Daza, M.L., Salaroglio, I.C., Kopecka, J., Garzòn, R., Couraud, P.-O., Ghigo, D., Riganti, C., 2014.
678 The cross-talk between canonical and non-canonical Wnt-dependent pathways regulates P-
679 glycoprotein expression in human blood–brain barrier cells. J. Cereb. Blood Flow Metab. 34, 1258–
680 1269. doi:10.1038/jcbfm.2014.100

681 Pisani, D., Pett, W., Dohrmann, M., Feuda, R., Rota-Stabelli, O., Philippe, H., Lartillot, N., Wörheide,
682 G., 2015. Genomic data do not support comb jellies as the sister group to all other animals. Proc.
683 Natl. Acad. Sci. 112, 15402–15407. doi:10.1073/pnas.1518127112

684 Plageman, T.F., Chauhan, B.K., Yang, C., Jaudon, F., Shang, X., Zheng, Y., Lou, M., Debant, A.,
685 Hildebrand, J.D., Lang, R.A., 2011. A Trio-RhoA-Shroom3 pathway is required for apical constriction
686 and epithelial invagination. Development 138, 5177–5188. doi:10.1242/dev.067868

687 Podar, K., Raab, M.S., Tonon, G., Sattler, M., Barilà, D., Zhang, J., Tai, Y.-T., Yasui, H., Raje, N.,
688 DePinho, R.A., 2007. Up-regulation of c-Jun inhibits proliferation and induces apoptosis via caspase-
689 triggered c-Abl cleavage in human multiple myeloma. Cancer Res. 67, 1680–1688.

690 Potin, S., Bertoglio, J., Bréard, J., 2007. Involvement of a Rho-ROCK-JNK pathway in arsenic trioxide-
691 induced apoptosis in chronic myelogenous leukemia cells. FEBS Lett. 581, 118–124.
692 doi:10.1016/j.febslet.2006.12.016

693 Reed, R.A., Womble, M.A., Dush, M.K., Tull, R.R., Bloom, S.K., Morckel, A.R., Devlin, E.W., Nascone-
694 Yoder, N.M., 2009. Morphogenesis of the primitive gut tube is generated by Rho/ROCK/myosin II–
695 mediated endoderm rearrangements. Dev. Dyn. 238, 3111–3125. doi:10.1002/dvdy.22157

696 Renard, E., Gazave, E., Fierro-Constain, L., Schenkelaars, Q., Ereskovsky, A., Vacelet, J., Borchiellini, C.,
697 2013. Porifera (Sponges): Recent Knowledge and New Perspectives, in: eLS. John Wiley & Sons, Ltd.

698 Richards, G.S., Degnan, B.M., 2009. The Dawn of Developmental Signaling in the Metazoa. Cold
699 Spring Harb. Symp. Quant. Biol. 74, 81–90. doi:10.1101/sqb.2009.74.028

700 Riento, K., Ridley, A.J., 2003. Rocks: multifunctional kinases in cell behaviour. Nat. Rev. Mol. Cell Biol.
701 4, 446–456. doi:10.1038/nrm1128

702 Riesgo, A., Farrar, N., Windsor, P.J., Giribet, G., Leys, S.P., 2014. The analysis of eight transcriptomes
703 from all Porifera classes reveals surprising genetic complexity in sponges. Mol. Biol. Evol. msu057.
704 doi:10.1093/molbev/msu057

705 Rivera, A., Winters, I., Rued, A., Ding, S., Posfai, D., Cieniewicz, B., Cameron, K., Gentile, L., Hill, A.,
706 2013. The evolution and function of the Pax/Six regulatory network in sponges: Pax/Six genes in
707 freshwater sponges. Evol. Dev. 15, 186–196. doi:10.1111/ede.12032

708 Ryan, J.F., Pang, K., Schnitzler, C.E., Nguyen, A.-D., Moreland, R.T., Simmons, D.K., Koch, B.J., Francis,
709 W.R., Havlak, P., Smith, S.A., Putnam, N.H., Haddock, S.H.D., Dunn, C.W., Wolfsberg, T.G., Mullikin,
710 J.C., Martindale, M.Q., Baxevanis, A.D., 2013. The Genome of the Ctenophore Mnemiopsis leidyi and
711 Its Implications for Cell Type Evolution. Science 342, 1242592. doi:10.1126/science.1242592

712 Schlessinger, K., Hall, A., Tolwinski, N., 2009. Wnt signaling pathways meet Rho GTPases. Genes Dev.
713 23, 265–277. doi:10.1101/gad.1760809

714 Schulte, G., 2010. International Union of Basic and Clinical Pharmacology. LXXX. The Class Frizzled
715 Receptors. Pharmacol. Rev. 62, 632–667. doi:10.1124/pr.110.002931

716 Semenov, M.V., Habas, R., MacDonald, B.T., He, X., 2007. SnapShot: Noncanonical Wnt Signaling
717 Pathways. Cell 131, 1378.e1–1378.e2. doi:10.1016/j.cell.2007.12.011

718 Shaulian, E., Karin, M., 2001. AP-1 in cell proliferation and survival. Oncogene 20, 2390–2400.
719 doi:10.1038/sj.onc.1204383

720 Sherrard, K., Robin, F., Lemaire, P., Munro, E., 2010. Sequential Activation of Apical and Basolateral
721 Contractility Drives Ascidian Endoderm Invagination. Curr. Biol. 20, 1499–1510.
722 doi:10.1016/j.cub.2010.06.075

723 Srivastava, M., Begovic, E., Chapman, J., Putnam, N.H., Hellsten, U., Kawashima, T., Kuo, A., Mitros, T.,
724 Salamov, A., Carpenter, M.L., Signorovitch, A.Y., Moreno, M.A., Kamm, K., Grimwood, J., Schmutz, J.,
725 Shapiro, H., Grigoriev, I.V., Buss, L.W., Schierwater, B., Dellaporta, S.L., Rokhsar, D.S., 2008. The
726 Trichoplax genome and the nature of placozoans. Nature 454, 955–960. doi:10.1038/nature07191

727 Srivastava, M., Simakov, O., Chapman, J., Fahey, B., Gauthier, M.E.A., Mitros, T., Richards, G.S.,
728 Conaco, C., Dacre, M., Hellsten, U., Larroux, C., Putnam, N.H., Stanke, M., Adamska, M., Darling, A.,
729 Degnan, S.M., Oakley, T.H., Plachetzki, D.C., Zhai, Y., Adamski, M., Calcino, A., Cummins, S.F.,
730 Goodstein, D.M., Harris, C., Jackson, D.J., Leys, S.P., Shu, S., Woodcroft, B.J., Vervoort, M., Kosik, K.S.,
731 Manning, G., Degnan, B.M., Rokhsar, D.S., 2010. The Amphimedon queenslandica genome and the
732 evolution of animal complexity. Nature 466, 720–726. doi:10.1038/nature09201

733 Stankova, V., Tsikolia, N., Viebahn, C., 2015. Rho kinase activity controls directional cell movements
734 during primitive streak formation in the rabbit embryo. Dev. Camb. Engl. 142, 92–98.
735 doi:10.1242/dev.111583

736 Strekal, T.A., McDIFFETT, W.F., 1974. Factors affecting germination, growth, and distribution of the
737 freshwater sponge, Spongilla fragilis Leidy (Porifera). Biol. Bull. 146, 267–278.

738 Thompson, J.D., Higgins, D.G., Gibson, T.J., 1994. CLUSTAL W: improving the sensitivity of progressive
739 multiple sequence alignment through sequence weighting, position-specific gap penalties and weight
740 matrix choice. Nucleic Acids Res. 22, 4673–4680.

741 Tu, D., Li, Y., Song, H.K., Toms, A.V., Gould, C.J., Ficarro, S.B., Marto, J.A., Goode, B.L., Eck, M.J., 2011.
742 Crystal structure of a coiled-coil domain from human ROCK I. PLoS One 6, e18080.

743 Verdier, V., Settleman, J., others, 2006. Rho-kinase regulates tissue morphogenesis via non-muscle
744 myosin and LIM-kinase during Drosophila development. BMC Dev. Biol. 6, 38.

745 Wall, D.P., Fraser, H.B., Hirsh, A.E., 2003. Detecting putative orthologs. Bioinformatics 19, 1710–1711.
746 doi:10.1093/bioinformatics/btg213

747 Watanabe, T., Hosoya, H., Yonemura, S., 2007. Regulation of myosin II dynamics by phosphorylation
748 and dephosphorylation of its light chain in epithelial cells. Mol. Biol. Cell 18, 605–616.

749 Windsor, P.J., Leys, S.P., 2010. Wnt signaling and induction in the sponge aquiferous system:
750 evidence for an ancient origin of the organizer: Polarity in sponges. Evol. Dev. 12, 484–493.
751 doi:10.1111/j.1525-142X.2010.00434.x

752 Winter, C.G., Wang, B., Ballew, A., Royou, A., Karess, R., Axelrod, J.D., Luo, L., 2001. < i>
753 Drosophila</i> Rho-Associated Kinase (Drok) Links Frizzled-Mediated Planar Cell Polarity Signaling to
754 the Actin Cytoskeleton. Cell 105, 81–91.

755 Xu, N., Keung, B., Myat, M.M., 2008. Rho GTPase controls invagination and cohesive migration of the
756 Drosophila salivary gland through Crumbs and Rho-kinase. Dev. Biol. 321, 88–100.
757 doi:10.1016/j.ydbio.2008.06.007

758 Yu, Z., Liu, M., Fu, P., Xie, M., Wang, W., Luo, X., 2012. ROCK inhibition with Y27632 promotes the
759 proliferation and cell cycle progression of cultured astrocyte from spinal cord. Neurochem. Int. 61,
760 1114–1120. doi:10.1016/j.neuint.2012.08.003

761 Zimmerman, S.G., Thorpe, L.M., Medrano, V.R., Mallozzi, C.A., McCartney, B.M., 2010. Apical
762 constriction and invagination downstream of the canonical Wnt signaling pathway require Rho1 and
763 Myosin II. Dev. Biol. 340, 54–66. doi:10.1016/j.ydbio.2010.01.021

764

765

766

767

768

769

770

771

772

773

774

775

776

777

778

779

780

781

782

783

784

Figure Legends

Figure 1. Consensus tree of ROCK proteins in Poriferan lineages. Bayesian posterior probabilities and maximum likelihood support are indicated above and below each node, respectively. Asterisks instead of supporting values indicate that the topology was not retrieved in the maximum likelihood analysis. Poriferan species are underlined. Species abbreviations. Porifera: Aq. *Amphimedon queenslandica*; Av, *Aphrocalistes vastus*; Em, *Ephydatia muelleri*; Om, *Oopsacas minuta*; Oc, *Oscarella carmela*; Ol, *Oscarella lobularis*; Osp, *Oscarella sp*. and Sc, *Sycon ciliatum*. Cnidarians: *Hydra magnipapillata*. Bilateria: Ci, *Ciona intestinalis* and Hs, *Homo sapiens*.

Figure 2: Evolution of ROCK proteins and conservation of functional domains. Species abbreviations. Porifera: Aq. *Amphimedon queenslandica*; Av, *Aphrocalistes vastus*; Em, *Ephydatia muelleri*; Om, *Oopsacas minuta*; Oc, *Oscarella carmela*; Ol, *Oscarella lobularis*; Osp, *Oscarella sp*. and Sc, *Sycon ciliatum*. Cnidaria: *Hydra magnipapillata*. Lophotrochozoa: Cg, *Crassostrea gigas* and Sm, *Schmitea mediterranea*. Ecdysozoans: Ll, *Loa loa*. Ambulacraria: Sp, *Strongylocentrotus purpuratus*. Vertebrates: Hs, *Homo sapiens*. Protein scale: 200 amino-acids.

Figure 3: Developmental expression of *Rock*, *Dvl* and *Daam*. Sponges were hatched from gemmules in Streakal's media and collected at the desired developmental stage for RNA extraction. qRT-PCR was used to measure *Em-rock*, *Em-dvl* and *Em-daam* expression (n=4) and was normalized by *Em-ef1* expression (n=4). Three main stages for each gene were discriminated by a Friedman test ($p<0.006$, $p<0.006$ and $p<0.003$, respectively) and a Nemenyi procedure.

Figure 4: Bacterially expressed Em ROCK kinase domain displays kinase activity. FLAG- and 6xHis-tagged ROCK kinase domain (amino acids 2-415) (A) could be expressed in bacteria and affinity-purified to high purity, as visualized by Coomassie staining of an SDS-PAGE gel (B). Purified fractions displayed concentration-dependent kinase activity (C), and were inhibited by the known ROCK inhibitors Y-27623 and GSK429286A in a concentration-dependent manner (D) *in vitro*. Graphs are representative of >3 trials from different protein preparations. Error bars represent SEM of replicates within a trial.

Figure 5. Exposure to Y-27632 induced growth zone aberrance and prevent aquiferous system development. A. Percentage of gemmules showing abnormal growth shape when treated with Y-27632. The significance of results were evaluated by Fisher's exact tests (***, P<0.001). **B.** Photos from above comparing the normal development of *E. muelleri* gemmules (G) to those of gemmules treated with Y-27632 over 72h. 24h old untreated sponges have a roughly circular body shape whereas treated sponges show outgrowth formation of the basal pinacoderm layer (arrowhead). 48h and 72h old untreated sponges have a complete aquiferous system with canals (C) and osculum (Os) whereas they are not distinguishable in treated sponges. However, 4µm cross sections revealed spicule (S) and choanocyte chambers (Cc) in gemmules exposed to 10µM Y27632 during 72h. Scales: 500, 500, 500 and 25µm, respectively. **C.** Percentage of gemmules without osculum when treated with Y-27632. The significance of results were evaluated by Fisher's exact tests (***, P<0.001).

Figure 7. Exposure to GSK429286A induced growth zone aberrance and prevent aquiferous system development. A. Percentage of gemmules showing abnormal growth shape when treated with GSK429286A. The significance of results were evaluated by Fisher's exact tests (***, P<0.001). **B.** Photos from above showing aberrations in *E. muelleri*

development from gemmules (G) by treating with different concentration of GSK429286A over 48h. 24h old treated sponges showed flattened, expanded and non-circular body shape at lowest concentrations (10µM and 25µM), whereas small outgrowths were observed at 50µM (arrowhead). Although few sponges with oscula (Os) were observed after 48h at 10µM, no oscula were observed in sponges cultivated with 25µM and 50µM. Scale: 500µm. **C.** Percentage of gemmules without osculum when treated with GSK429286A. The significance of results were evaluated by Fisher's exact tests (*, P<0.05; **, P<0.01 and ***, P<0.001).

Figure 8. Schematic representation of potential cross-talks between Wnt/β-catenin, Rho/Rock and JNK/JUN pathways. According to previous studies, the activation of the Wnt/β-catenin module induces ectopic formation of osculum and ostia (Lapébie et al., 2009; Windsor and Leys, 2010). Here we showed that the ROCK inhibition certainly prevents the morphogenesis of the aquiferous system. Moreover, the down-regulation of Em-Dishevelled (Dvl) and the over-expression of Em-Cyclin D suggest that ROCK inhibition affects all Wnt pathways while it may promote JNK/JUN module (Schulte, 2010; Semenov et al., 2007).

Figure 9. Relative gene expression levels following exposure to 10µM of Y-27632 over 72h. Treated sponges (n=12) were collected and used for RNA extraction. qRT-PCR was used to measure *Em-cyclin D* expression (*Em-ccnD*, n=2) and *Em-dishevelled* expression (*Em-dvl*, n=3). *Elongation factor 1 alpha* (*Em-ef1*) (n=3), *Em-piwi* (n=2) and *Em-actin* (n=2) expressions were also quantified as expression controls.

Figure 10: No effect of Y27632 treatment on 1 week old juvenile sponges (20µM treatment for 3 days). Abbreviations. C, canal; Cc, Choanocyte chamber; G, gemmule and Os, osculum. Scale: 500µm, 500µm and 50µm respectively.

Figure 1

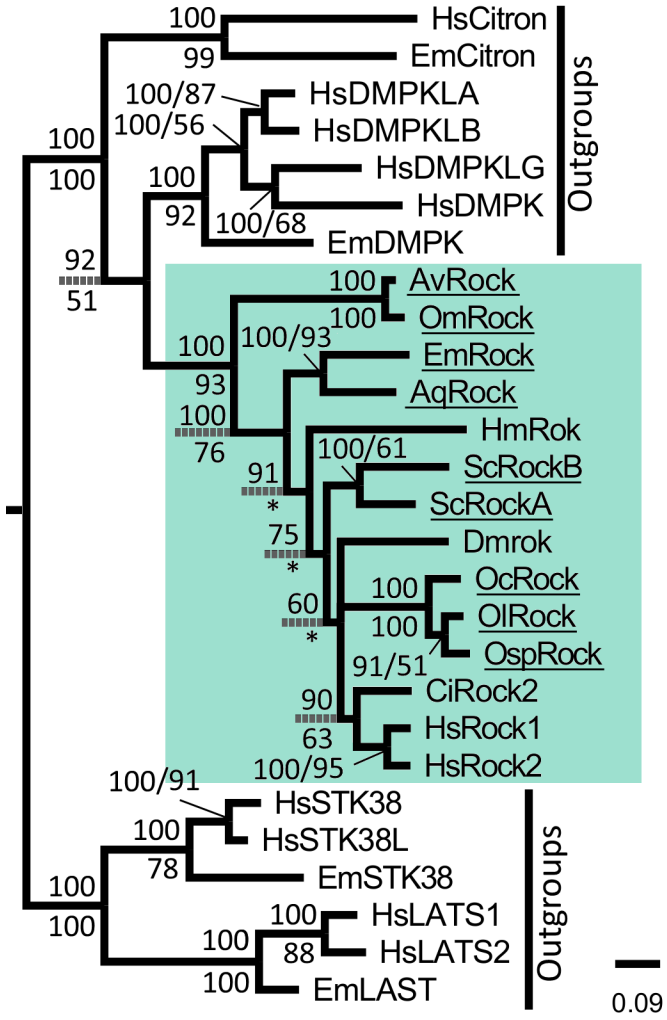
HsCitron
EmCitron
HsDMPKLA
HsDMPKLB
HsDMPKLG
HsDMPK
EmDMPK
Outgroups
AvRock
OmRock
EmRock
AqRock
HmRok
ScRockB
ScRockA
Dmrok
OcRock
OlRock
OspRock
CiRock2
HsRock1
HsRock2
HsSTK38
HsSTK38L
EmSTK38
HsLATS1
HsLATS2
EmLAST
Outgroups
0.09

Figure 2

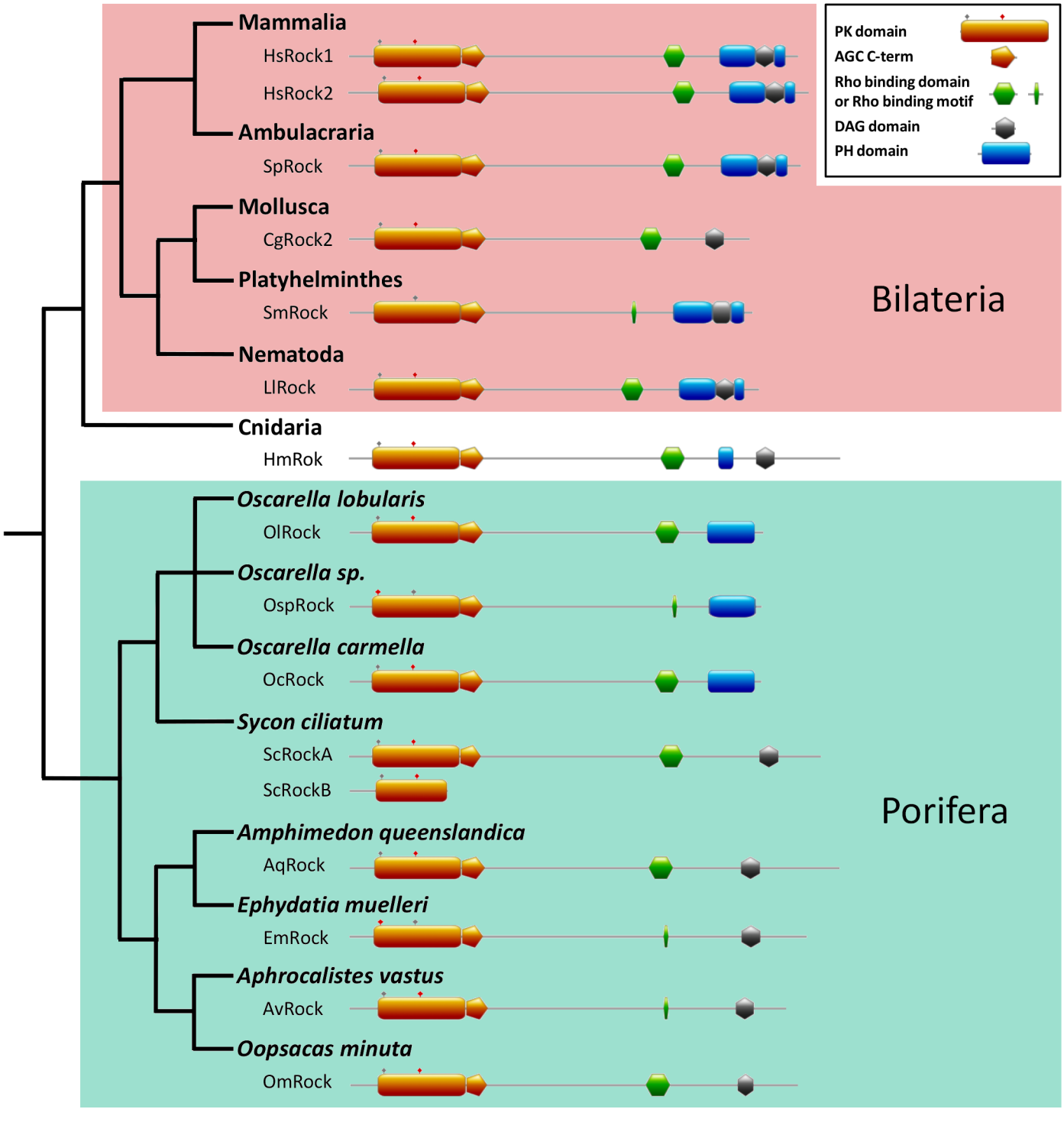
Mammalia
HsRock1
HsRock2
Ambulacraria
SpRock
Mollusca
CgRock2
Platyhelminthes
SmRock
Nematoda
LlRock
Bilateria
Cnidaria
HmRok
PK domain
AGC C-term
Rho binding domain
or Rho binding motif
DAG domain
PH domain
Oscarella lobularis
OlRock
Oscarella sp.
OspRock
Oscarella carmella
OcRock
Sycon ciliatum
ScRockA
ScRockB
Amphimedon queenslandica
AqRock
Ephydatia muelleri
EmRock
Aphrocalistes vastus
AvRock
Oopsacas minuta
OmRock
Porifera

Figure 3

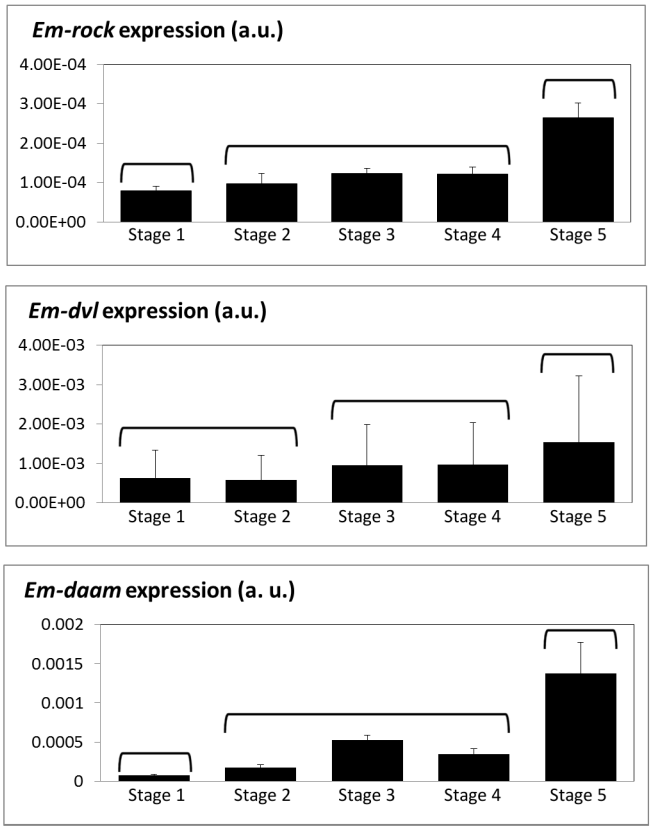
Em-rock expression (a.u.)
4.00E-04
3.00E-04
2.00E-04
1.00E-04
0.00E+00
Stage 1
Stage 2
Stage 3
Stage 4
Stage 5
Em-dvl expression (a.u.)
4.00E-03
3.00E-03
2.00E-03
1.00E-03
0.00E+00
Stage 1
Stage 2
Stage 3
Stage 4
Stage 5
Em-daam expression (a. u.)
0.002
0.0015
0.001
0.0005
0
Stage 1
Stage 2
Stage 3
Stage 4
Stage 5

Figure 4

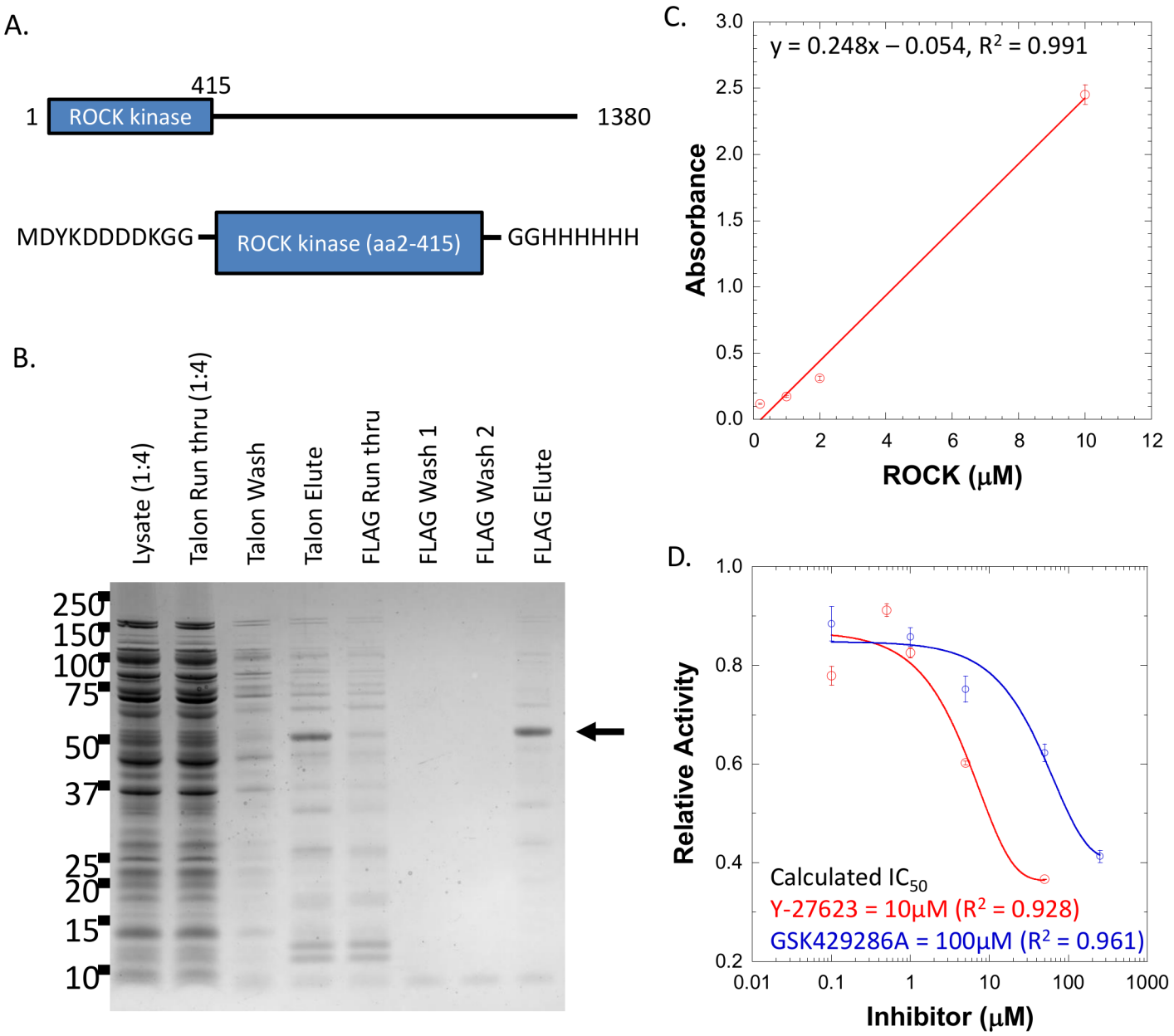
A.
415
1
ROCK kinase
1380
MDYKDDDDKGG
ROCK kinase (aa2-415)
GGHHHHHH
B.
Lysate (1:4)
Talon Run thru (1:4)
Talon Wash
Talon Elute
FLAG Run thru
FLAG Wash 1
FLAG Wash 2
FLAG Elute
250
150
100
75
50
37
25
20
15
10
C.
y = 0.248x – 0.054, R2 = 0.991
Absorbance
ROCK (μM)
D.
Relative Activity
Inhibitor (μM)
Calculated IC50
Y-27623 = 10μM (R2 = 0.928)
GSK429286A = 100μM (R2 = 0.961)

Figure 5

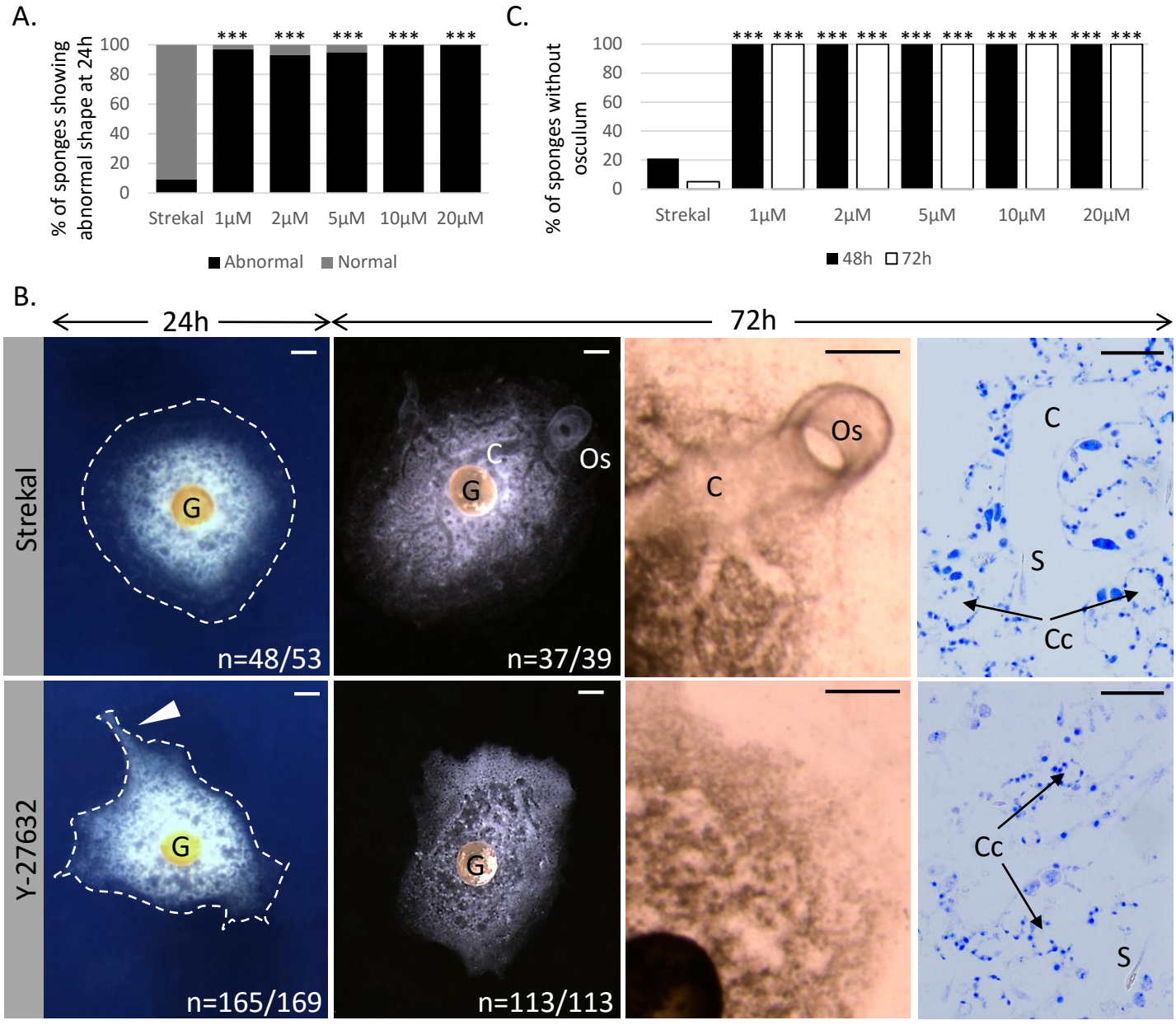
A.
% of sponges showing abnormal shape at 24h
100
80
60
40
20
0
***
Strekal
1μM
2μM
5μM
10μM
20μM
Abnormal
Normal
C.
% of sponges without osculum
48h
72h
B.
24h
72h
Strekal
Y-27632
G
C
Os
S
Cc
n=48/53
n=37/39
n=165/169
n=113/113

Figure 6

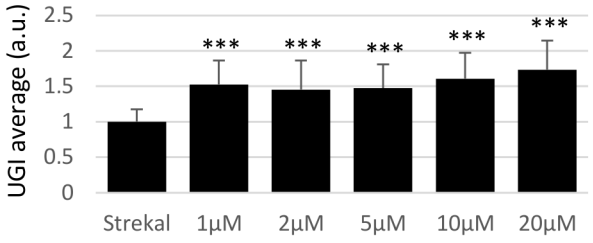

Figure 7

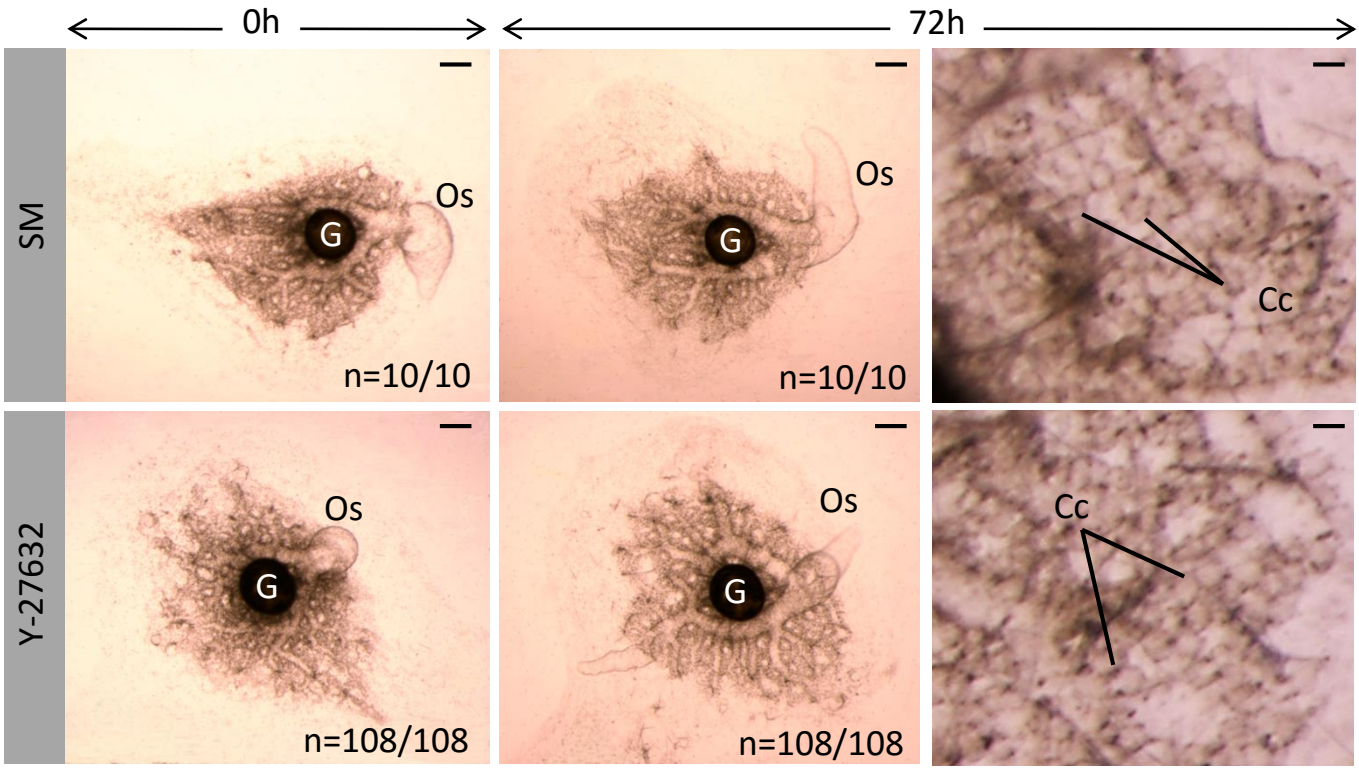

Figure 8

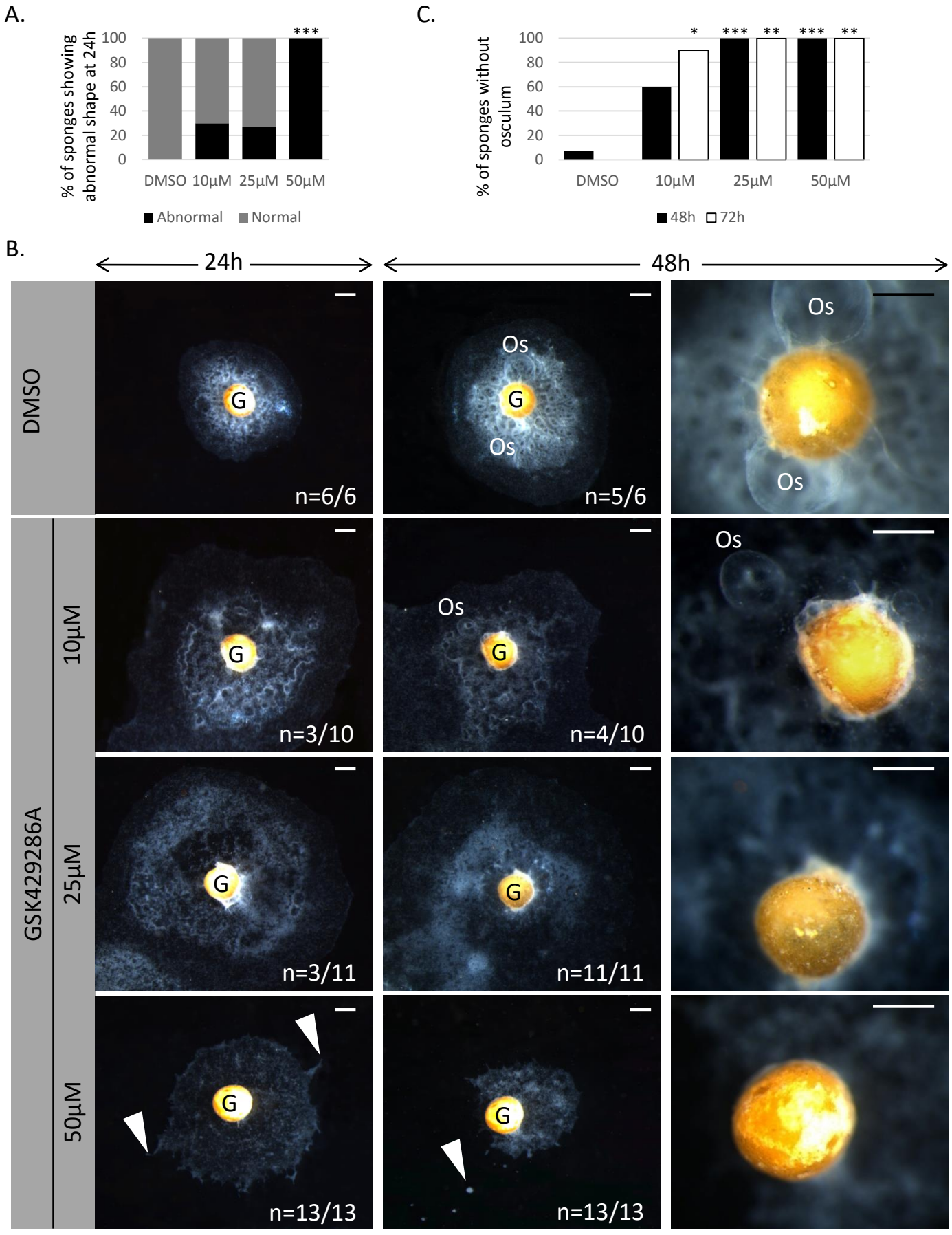
A.
% of sponges showing abnormal shape at 24h
100
80
60
40
20
0
***
DMSO
10µM
25µM
50µM
Abnormal
Normal
C.
% of sponges without osculum
100
80
60
40
20
0
*
***
**
***
**
DMSO
10µM
25µM
50µM
48h
72h
B.
24h
48h
DMSO
GSK429286A
10µM
25µM
50µM
G
Os
n=6/6
n=5/6
n=3/10
n=4/10
n=3/11
n=11/11
n=13/13
n=13/13

Figure 9

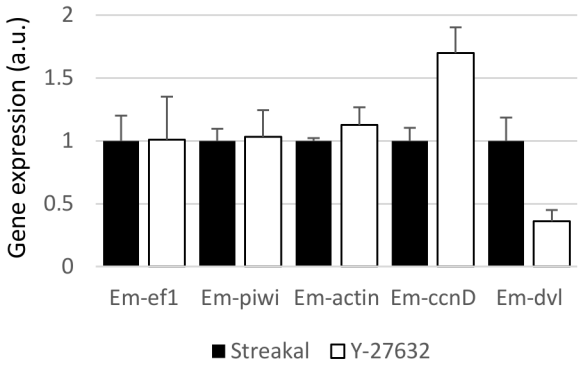
Gene expression (a.u.)
2
1.5
1
0.5
0
Em-ef1
Em-piwi
Em-actin
Em-ccnD
Em-dvl
Streakal
Y-27632

Figure 10

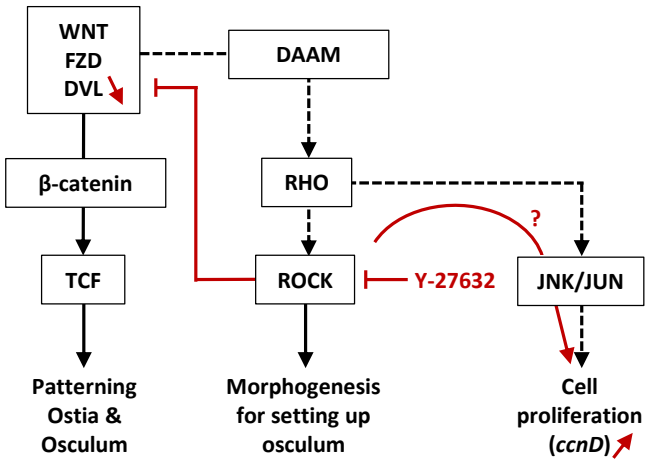
WNT
FZD
DVL
DAAM
β-catenin
RHO
?
TCF
ROCK
Y-27632
JNK/JUN
Patterning
Ostia &
Osculum
Morphogenesis
for setting up
osculum
Cell
proliferation
(ccnD)